HHS Public Access

Author manuscript

Mol Imaging Biol. Author manuscript; available in PMC 2023 April 01.

Published in final edited form as:

Mol Imaging Biol. 2022 April ; 24(2): 280–287. doi:10.1007/s11307-021-01667-0.

In Vivo Evaluation of Near-Infrared Fluorescent Probe for TIM3 Targeting in Mouse Glioma

Michael Zhang, MD[1,2], **Quan Zhou, PhD**[1,3], **Chinghsin Huang, PhD**[2], **Carmel T. Chan, PhD**[2], **Wei Wu, PhD**[2], **Gordon Li, MD**[1], **Michael Lim, MD**[1], **Sanjiv S. Gambhir, MD PhD**[2], **Heike E. Daldrup-Link, MD**[2,*]

[1.]Department of Neurosurgery, Stanford University, Stanford, CA

[2.]Department of Radiology, Stanford University, Stanford, CA

[3.]Department of Otolaryngology-Head and Neck Surgery, Stanford University, Stanford, CA

Abstract

Purpose: Current checkpoint inhibitor immunotherapy strategies in glioblastoma are challenged by mechanisms of resistance including an immunosuppressive tumor microenvironment. T cell immunoglobulin domain and mucin domain 3 (TIM3) is a late phase checkpoint receptor traditionally associated with T cell exhaustion. We apply fluorescent imaging techniques to explore feasibility of *in vivo* visualization of the immune state in a glioblastoma mouse model.

Procedures: TIM3 monoclonal antibody was conjugated to a near-infrared fluorescent dye, IRDye-800CW (800CW). The TIM3 experimental conjugate and isotype control were assessed for specificity with immunofluorescent staining and flow cytometry in murine cell lines (GL261 glioma and RAW264.7 macrophages). C57BL/6 mice with orthotopically implanted GL261 cells were imaged *in vivo* over four days after intravenous TIM3-800CW injection to assess tumor specific uptake. Cell specific uptake was then assessed on histologic sections.

Results: The experimental TIM3-800CW, but not its isotype control, bound to RAW264.7 macrophages *in vitro*. Specificity to RAW264.7 macrophages and not GL261 tumor cells was quantitatively confirmed with the corresponding clone of TIM3 on flow cytometry. *In vivo* fluorescence imaging of the 800CW signal was localized to the intracranial tumor and significantly higher for the TIM3-800CW cohort, relative to non-targeting isotype control, immediately after tail vein injection and for up to 48 hours after injection. Resected organs of tumor bearing mice showed significantly higher uptake in the liver and spleen. TIM3-800CW was seen to co-stain with CD3 (13%), CD11b (29%), and CD206 (26%).

[*]Corresponding author: Heike E. Daldrup-Link, MD, PhD, 725 Welch Road, Rm 1665, Stanford, CA 94305-5614, Ph: (650) 723-8996, Fax: (650) 725-8957, heiked@stanford.edu.

Author Contributions

Conception and Design: MZ, QZ, CTC, GL, ML, SSG, HED
Acquisition of Data/Materials: MZ, QZ, CH, WW, CTC, SSG, HED
Analysis of Data: MZ, QZ, CH, CTC
Drafting of Manuscript: MZ
Critical Revision: QZ, CH, CTC, WW, GL, ML, SSG, HED
Final Approval: MZ, QZ, CH, CTC, WW, GL, ML, SSG, HED
Agreement of Accountability: MZ, QZ, CH, CTC, WW, GL, ML, SSG, HED

Conflict of Interest: The authors declare that they have no conflict of interest.

Conclusions: We propose fluorescent imaging of immune cell imaging as a potential strategy for monitoring and localizing immunologically relevant foci in the setting of brain tumors. Alternative markers and target validation will further clarify the temporal relationship of immunosuppressive effector cells throughout glioma resistance.

Keywords

checkpoint inhibitor; fluorescence; glioblastoma; immune suppression; TIM3

Introduction

Glioblastoma's response to checkpoint inhibitors (CPI) such as anti-CTLA-4 and anti-PD1 has been particularly challenged by an immunosuppressive environment.[1-2] Inhibitory cytokines, anti-inflammatory immune cells, and compensatory immune checkpoints have all limited the successes of monotherapy as well as combination CPI therapies.[3] TIM3 (T cell immunoglobulin domain and mucin domain-3) has emerged among a collection of late-appearing checkpoint molecules that signal T cell exhaustion.[4-5] During this immune progression, T cell stimulation is unable to achieve expected T cell activation or proliferation to generate a protective immune response. Preclinical studies have shown that incorporating anti-TIM3 and other CPI therapies to protocols can augment GBM treatment.[5]

Fluorescence imaging has also emerged as a new management technique for glioblastoma. Intra-operative use of 5-ALA has enhanced the visual localization of high-grade glioma and improved outcomes based on the targeting of the tumors' upregulated heme biosynthesis pathway.[6] However, such labeling has been primarily devoted to delineating tumor boundary, without further characterization of tissue properties. Combining fluorescence imaging techniques and selective biomolecular markers can provide additional functional assessments of the underlying glioma immunology.[7] In particular, targeted molecular imaging could characterize the immunosuppressive tumor microenvironment and predict responsiveness to CPI therapies.[8-10]. If progressive resistance to early CPI therapies is encountered, later stage targets will also merit evaluation. Thus, we assess the feasibility of visualizing a TIM3 antibody conjugated to a near infrared (NIR) fluorescent dye in an orthotopic glioblastoma mouse model as a first step for *in vivo* monitoring.

Materials and Methods

Cells

Mouse macrophage RAW 264.7 cell lines (ATCC; Manassas, VA) and mouse glioma-derived, luciferase-expressing GL261 (NCI: Bethesda, MD) labeled in-house with firefly luciferase were maintained in Dulbecco's Modified Eagle Medium + 10% fetal bovine serum + 1% anti-mycotic and penicillin-streptomycin at 37°C in a humidified incubator maintained at 5% CO_2 and 5% O_2. All cultures were subjected to mycoplasma testing and confirmed negative prior to use. A listing of all catalogue numbers and manufacturers are available in Supplementary Table 1.

Flow cytometry

Cells were pre-treated with Fc block (anti-CD16/32; 101302, BioLegend), washed, and stained with Live/Dead Aqua (Thermo Fisher). Cells were stained for TIM3 (clone RMT3-23, 119716, BioLegend; 1:200). Signals were acquired on the LSR II flow cytometer (BD). All FACS data were analyzed using BD FACSDiva software. Nonviable cells were excluded by forward versus side scatter analysis and Live/Dead Aqua staining.

TIM3 Small Inhibitory RNA (siRNA)

RAW 264.7 cells and GL261 cells were seeded (3×10^5) in 6-well plates culture media the day prior to transfection with lipofectamine RNAiMAX (13778030, Thermo Fisher) according to the manufacturer's instructions. siRNA sequence targeting TIM3 were bioinformatically designed (Stealth siRNA, 1320001, Thermo Fisher). Scrambled siRNA with medium GC-content was used as a control (12935300, Thermo Fisher). siRNA was added at a final concentration of 50 nM, and TIM3 expression was measured at 48 hours after transfection by flow cytometry.

Synthesis of IRDye800CW Conjugates

TIM3-IRDye800CW was prepared by conjugating IRDye800CW (800CW) succinimidyl ester (928-38040, LI-COR Biosciences) to either rat IgG2a monoclonal antibody (IgG mAb; BE0089, Bio X Cell) or TIM3 monoclonal antibody (TIM3 mAb; BE0115, Bio X Cell) according to the manufacturer's instructions. Briefly, 2 mg/mL of either IgG mAb or TIM3 mAb in PBS (pH 7.0) and aqueous 800CW succinimidyl ester (3.4 mM) were combined and rotated at room temperature for 2 hours. The resulting solution was purified by Zeba Spin Desalting Columns (Thermo Fisher) centrifugal with 7.0-kDa size exclusion resins. The fluorescent probe was submitted for spectrometer and mass spectrometry analysis using the SpectraMax M2e System (Molecular Devices) and TOF/TOF 5800 System (SCIEX), respectively.

Immunofluorescence analysis

Cells were grown on Nunc Lab-Tek II chamber slides (Thermo Fisher) in culture media the day prior to staining. They were incubated overnight at 4°C with either IgG-800CW or TIM3-800CW antibody conjugates. Slides were counterstained with 4', 6-diamidino-2-phenylindole (DAPI, 300nM; D1306, Invitrogen), and imaged using a custom-built fluorescence microscope (Leica).[11] Mean fluorescence intensities (MFIs) were normalized to that of the negative sample using ImageJ (v1.53).

For immunofluorescence colocalization analysis on brain tumor tissue, deparaffinized and rehydrated tissue slices were steamed 20 minutes in antigen retrieval citra plus solution (NC9576335, Thermo Fisher). Slices were blocked with 5% goat serum (2939149, CELLect) in PBS-T for 30 minutes. The slides were subsequently incubated with primary antibodies at 4°C overnight. Following primary antibodies were used: Rat anti-mouse TIM3 (MCA5790GA, Bio Rad, 1:100), Rabbit anti-mouse CD3 (ab5690, Abcam, 1:100), and Rabbit anti-mouse CD11b (ab133357, Abcam, 1:1000), Rabbit anti-mouse CD206 (ab64693, Abcam, 1:2000). Secondary antibodies were stained for 1 hour at room temperature: Goat anti-rabbit IgG Alexa Fluor 594 (A-11012, Thermo Fisher, 1:500) and

goat anti-rat IgG Alexa Fluor 488 (A-11006, Thermo Fisher, 1:500). DAPI staining was used for nuclei staining. The immunofluorescence was observed under Keyence microscopy and analyzed with ImageJ 2.1.0.

Orthotopic brain tumor mouse model

All applicable institutional and/or national guidelines for the care and use of animals were followed. Animal experiments were carried out in accordance with Stanford University Institutional Animal Care and Use Committee guidelines (protocol #37129). Orthotopic brain tumor mouse model were established in six- to eight-week-old female C57BL/6 mice (000058, Jackson Laboratory) as previously described.[12] GL261 cells were stereotactically implanted (1 x 10^6 cells in 2 μL) into the striatum of the right brain hemisphere using the following coordinates: 2 mm posterior to the bregma, 2 mm lateral to the midline and 3 mm deep with regards to the surface of the brain. Tumor growth was monitored via bioluminescence imaging (IVIS Spectrum, PerkinElmer) after intraperitoneal injection of D-Luciferin (firefly) potassium salt solution (Biosynth, 15 mg/ml, 0.139 g luciferin per kg body weight), and total photon flux (photons/sec) was quantified using Living Image (v4.5.5, PerkinElmer).

NIR imaging

Tumor-bearing mice were randomized and injected with either TIM3-800CW (N=4) and IgG-800CW (N=4) fluorescent conjugates (concentration 2 mg/mL; 0.325 mg/mouse). Mice were imaged in 24-hour intervals over a period of up to 4 days. Time of injection (post-implantation day 11) was selected based on tumor growth rate and anticipated morbidity. *In vivo* conjugate binding was monitored via fluorescence imaging (excitation/emission 745/800 nm, IVIS Spectrum, PerkinElmer) with image acquisition parameters: small binning, f-stop 2, and 3 seconds of exposure. Pharmacokinetics were measured based on tumor MFI, and tumor to background ratio (TBR) calculated as MFI in each tumor region of interest (ROI), divided by MFI of normal tissue (Supplementary Figure 1).

Organs from control and experimental cohorts were collected from euthanized mice on Day 3 or 4, based on clinical morbidity or on reaching the predefined trial endpoint, respectively. *Ex vivo* imaging was evaluated in a NIR florescence imager (excitation/emission: 785/ 820 nm, resolution = 85 μm; Pearl Trilogy Imaging System, LI-COR Biosciences) and processed with ImageStudio (v5.2, LI-COR Biosciences). TBR was defined as the MFI of either the fluorescently enhancing tumor or the whole organ divided by the MFI of histologically negative tissue (muscle).

Mouse organs were formalin-fixed overnight, paraffin-embedded, and sectioned (4 μm thick). To assess tumor specificity of conjugate antibodies, fluorescence images of sections were scanned in a closed-field NIR imaging device, Odyssey CLx (excitation/emission: 785/ 820 nm, resolution = 21 μm; LI-COR Biosciences) and processed with ImageStudio. TBR was defined as the MFI of the tumor as delineated on hematoxylin and eosin staining divided by the MFI of contralateral brain. To assess for cell specificity, brain sections were rehydrated and counterstained with DAPI (300 nM, Invitrogen) before they were imaged with Keyence microscopy (excitation/emission 740/780).

Statistical analysis

Data are expressed as mean ± standard error of the mean (SEM). Cohorts were compared by Mann-Whitney U test (R Studio 1.2.5033) as appropriate. Statistical significance was defined at $P < 0.05$.

Results

TIM3-800CW conjugate detects TIM3 expression in vitro

Following conjugation of the 800CW to the experimental probe, TIM3 mAb (clone RMT3-23), and the IgG isotype control, the conjugates were used to stain the RAW264.7 macrophage cell line by immunofluorescence. NIR microscopy confirmed that only TIM3-800CW bound to RAW264.7 cells (Figure 4). Expression of TIM3 on RAW 264.7 was validated by flow cytometry using commercially labeled antibodies of the same clone (Supplementary Figure 2). Specificity of the TIM3 clone was further assessed by siRNA knockdown against TIM3, whereafter transfection, a decreased expression was observed (74.54 ± 2.69 vs 28.88 ± 2.55 MFI, p = 0.0079, Mann-Whitney U). TIM3 expression levels at baseline and following siRNA knockdown were also assessed for GL261 mouse-derived glioma cell. Expression was not significantly lower (7.98 ± 2.89 vs 3.37 ± 0.23 MFI, p = 0.6905, Mann-Whitney U).

TIM3-800CW detects GL261 in mice in vivo and ex vivo on NIR fluorescence imaging

Mice with orthotopically implanted, syngeneic GL261 cells were administered either TIM3-800CW (n = 4) or IgG-800CW (n = 4). Fluorescence was detected intracranially within one hour following tail vein injection and corresponded to the sites of tumor implantation (Figure 1, Supplementary Figure 3). MFI was highest at the initial time of injection with a TBR of 1.7 ± 0.09 vs 1.2 ± 0.1 (p = 0.0286, Mann-Whitney U) between TIM3-800CW and IgG-800CW cohorts. MFI remained higher than control for all time points and declined over time. There was no statistically significant difference between TIM3-800CW and IgG-800CW cohorts at 72 hours after administration (1.3 ± 0.5 vs 1.1 ± 0.4, p = 0.0571, Mann-Whitney U). Fluorescent signal continued to be visible at the tumor site over 96 hours, at which point MFI had diminished by approximately 23.5% in the remaining TIM3-800CW cohort.

Organs from the TIM3-800CW cohort showed *ex vivo* TIM3-800CW fluorescent signals in brain, liver, and kidney with MFI > 10 when normalized to muscle (Figure 2). The brain TBR MFI signal was higher in the TIM3-800CW cohort compared to the IgG-800CW cohort (30.1 ± 5.6 vs 13.4 ± 3.7, p = 0.0571, Mann-Whitney U, Supplementary Figure 4). 800CW signal was also significantly higher for the TIM3-800CW cohort for liver (20.05 ± 0.88 vs 7.7 ± 0.13, p = 0.0286, Mann-Whitney U) and spleen (5.7 ± 0.16 vs 3.3 ± 0.04, p = 0.0286, Mann-Whitney U). Corresponding high resolution histologic sections were also assessed, in which TIM3-800CW signal accumulation was detected within the tumor boundary (Figure 4). The segmented area confirmed a higher MFI normalized to contralateral brain for TIM3-800CW as compared to IgG-800CW. (Supplementary Table 2, Figure 4).

Specificity at the cellular level was further confirmed by immunofluorescent microscopy (Supplementary Figure 5). CD11b (general macrophages), CD206 (M2-type macrophages), and CD3 (T cells) co-stained with TIM3 in ex vivo brain tumor tissues. Immunofluorescent colocalization images revealed that 13% of T cells co-expressed TIM3, while 29% of macrophages and 26% of M2-type macrophages co-expressed TIM3.

Discussion

The use of intra-operative imaging has become standard of care for management of glioblastoma, with current cytoreduction strategies primarily focusing on identifying tumor margins. In this study we look to alternatively label one of the key drivers of tumor persistence and recurrence, namely, immune suppression via TIM3. The labeling strategy in the NIR confirms that TIM3 provides potential sensitivity and specificity needed for intravital fluorescent detection.

TIM3 Labeling for Monitoring Progression

Our *in vivo* results demonstrated early tumor labeling that persisted for at least two days. We suspect that rapid drug uptake in brain tumors was due to a prominent contribution by the enhanced permeability and retention effect.[13] This is further evidenced by detection of some signal within the tumor in the IgG control cohort. Nevertheless, there is a strong differential in signal intensity between the two treatment arms to support specificity by the experimental TIM3-800CWs. Moreover, immunofluorescent staining of brain sections suggested cellular uptake unrelated to vascular or interstitial territories. This *in vivo* trial intentionally investigated our labeling strategy in a late-stage tumor to maximize the potential of detecting TIM3 presence.[5] Thus, future studies will need to examine the *in vivo* signal for early phase and recurrent tumors.

Clinically, the intra-vital fluorescent-labeling strategy presented is likely not replicable considering the thickness of the human skull but can be visualized intra-operatively as demonstrated in prior intracranial applications of conjugated 800CW.[14] Alternatively, TIM3 antibodies can be radiolabeled for positron emission tomography. This strategy, albeit expensive, would enable a useful means of non-invasive monitoring of treatment response, which is especially important with current CPI therapies since anti-PD1 has not shown sustained clinical benefit (Checkmate 143, 498 and 548).[15] The current work, if used non-invasively, can be valuable for determining the critical window at which to intervene. For example, if a failing regimen is rapidly detected and switched, this may halt recurrence and obviate future resection.

TIM3 Labeling for Translational Disruption of GBM Resistance

A related application involves using an immune marker such as TIM3 to identify extracranial sources of immunosuppressive cells. Although brain tumors are frequently cited as involving extracranially sourced immune cells such as regulatory T cells and macrophages, an important strategy could be to identify organs of origin to interfere with their intracranial entry. Our pharmacokinetic evaluation confirmed a strong role in hepatic clearance of TIM3-800CW; however, there was also evidence to suggest a differential

splenic signal. This is consistent with our understanding of the regulatory T cell escalations and should be considered in future iterations.[16-18] The fluorescent scanners for our intravital evaluation in this study were of limited sensitivity, but future options may consider capturing extracranial signals of immunosuppressive nodes for monitoring and clinical-decision making.

Although less practical for *ex vivo* intracranial analysis in the human setting, fluorescently labeled TIM3 still offers immune characterization of the intracranial space for stereotactic, intra-operative management. An important value of 5-ALA acid, beyond margin detection, is its property of accurate localization despite brain shift throughout a resection. The identification of focal, immunosuppressive tissue as proposed here would provide a valuable site selection strategy for adjunct therapies necessitating localized administration. Such would greatly benefit intra-cavitary applications of vaccine and gene therapies that need to co-localize or evade an immunogenic foci.[19] Even post-operatively, this topographical information may help guide radiation or focused ultrasound treatment planning.[20-23]

Limitations

As with all intracranial targeting of high-grade glioma, a major limitation is understanding how a candidate reagent will behave in the context of various levels of blood brain barrier disruption. We noticed areas of hemorrhage within certain histologic samples for the control cohort, which may have contributed to the magnitude of background signal. Thus, it is possible that in earlier stage tumors, where the blood brain barrier is more preserved the signal ratio of TIM3-800CW to IgG-800CW in treated lesions could be even higher than that seen here. If there is a reduced enhanced permeability and retention effect, then the tumor is perhaps less permissive of non-specific binding. Additionally, our *in vitro* flow cytometric analyses were unable to measure TIM3-800CW labeling as our flow cytometry units did not have detector for the necessary NIR spectrum. Therefore, we were required to consider alternative, qualitative visualizations.

Finally, this study remains an early-stage evaluation of how immunofluorescence can be used *in vivo* and for clinical applications. Additional follow-up studies of the dynamic range of TIM3 expression are needed. Probe activity ultimately must correlate with the underlying immunological state of the tumor as determined by its ability to guide clinical responsiveness. Although classically described as a marker of T cell exhaustion, we did see macrophage cell lines exhibit a proportionally greater coinciding positive signal. Prior work has also shown TIM3 expression on other cell populations, including several immune cells as well as glioblastoma.[5, 24-25] Even if the tumor population contributes to the positive TIM3 signal, we believe this to still be informative of the regionally immunosuppressed state.

Conclusions

Here we present early data demonstrating feasibility of non-invasive TIM3 imaging in mice for applications in glioblastoma. This was motivated by needs to assess current barriers in central nervous system CPI therapies, including timely identification and localization of immune suppression. Such labeling within glioblastoma for evaluation of therapeutic

responsiveness can potentially aid with selection of salvage regimens or intra-operative targets. Additional studies are warranted to expand the pharmacokinetic profile and confirm cell specificity. Meanwhile, alternative markers of immune suppression can be assessed by the same labeling strategies.

Supplementary Material

Refer to Web version on PubMed Central for supplementary material.

Funding:

MZ receives research funding from the National Institutes of Health (5T32CA009695-27, MPI).

References

1. Lim M, Xia Y, Bettegowda C, Weller M (2018) Current state of immunotherapy for glioblastoma. Nat Rev Clin Oncol 15:422–442. [PubMed: 29643471]
2. McGranahan T, Therkelsen KE, Ahmad S, Nagpal S (2019) Current State of Immunotherapy for Treatment of Glioblastoma. Curr Treat Options Oncol 20:24. [PubMed: 30790064]
3. Jackson CM, Choi J, Lim M (2019) Mechanisms of immunotherapy resistance: lessons from glioblastoma. Nat Immunol 20:1100–1109. [PubMed: 31358997]
4. Anderson AC, Joller N, Kuchroo VK (2016) Lag-3, Tim-3, and TIGIT: Co-inhibitory Receptors with Specialized Functions in Immune Regulation. Immunity 44:989–1004. [PubMed: 27192565]
5. Kim JE, Patel MA, Mangraviti A, et al. (2017) Combination Therapy with Anti-PD-1, Anti-TIM-3, and Focal Radiation Results in Regression of Murine Gliomas. Clin Cancer Res 23:124–136. [PubMed: 27358487]
6. Mazurek M, Kulesza B, Stoma F, Osuchowski J, Mańdziuk S, Rola R (2020) Characteristics of Fluorescent Intraoperative Dyes Helpful in Gross Total Resection of High-Grade Gliomas-A Systematic Review. Diagnostics (Basel) 10.
7. Zhou Q, van den Berg N, Rosenthal E, et al. (2021) EGFR-targeted intraoperative fluorescence imaging detects high-grade glioma with panitumumab-IRDye800 in a phase 1 clinical trial. Thernostics.
8. Du Y, Sun T, Liang X, et al. (2017) Improved resection and prolonged overall survival with PD-1-IRDye800CW fluorescence probe-guided surgery and PD-1 adjuvant immunotherapy in 4T1 mouse model. Int J Nanomedicine 12:8337–8351. [PubMed: 29200846]
9. Li L, Du Y, Chen X, Tian J (2018) Fluorescence Molecular Imaging and Tomography of Matrix Metalloproteinase-Activatable Near-Infrared Fluorescence Probe and Image-Guided Orthotopic Glioma Resection. Mol Imaging Biol 20:930–939. [PubMed: 29651576]
10. Wissler HL, Ehlerding EB, Lyu Z, et al. (2019) Site-Specific Immuno-PET Tracer to Image PD-L1. Mol Pharm 16:2028–2036. [PubMed: 30875232]
11. Nishio N, van den Berg NS, van Keulen S, et al. (2019) Optical molecular imaging can differentiate metastatic from benign lymph nodes in head and neck cancer. Nature communications 10:1–10.
12. Yecies D, Liba O, SoRelle ED, et al. (2019) Speckle modulation enables high-resolution wide-field human brain tumor margin detection and in vivo murine neuroimaging. Scientific reports 9:1–9. [PubMed: 30626917]
13. Prabhakar U, Maeda H, Jain RK, et al. (2013) Challenges and key considerations of the enhanced permeability and retention effect for nanomedicine drug delivery in oncology. AACR.
14. Zhou Q, Vega Leonel JCM, Santoso MR, et al. (2021) Molecular imaging of a fluorescent antibody against epidermal growth factor receptor detects high-grade glioma. Sci Rep 11:5710. [PubMed: 33707521]

15. Reardon DA, Brandes AA, Omuro A, et al. (2020) Effect of Nivolumab vs Bevacizumab in Patients With Recurrent Glioblastoma: The CheckMate 143 Phase 3 Randomized Clinical Trial. JAMA Oncol 6:1003–1010. [PubMed: 32437507]
16. Anderson AC, Anderson DE, Bregoli L, et al. (2007) Promotion of tissue inflammation by the immune receptor Tim-3 expressed on innate immune cells. Science 318:1141–1143. [PubMed: 18006747]
17. Cole KE, Ly QP, Hollingsworth MA, et al. (2020) Comparative phenotypes of peripheral blood and spleen cells from cancer patients. Int Immunopharmacol 85:106655. [PubMed: 32521493]
18. Velásquez-Lopera MM, Correa LA, García LF (2008) Human spleen contains different subsets of dendritic cells and regulatory T lymphocytes. Clin Exp Immunol 154:107–114. [PubMed: 18727627]
19. Koks CA, De Vleeschouwer S, Graf N, Van Gool SW (2015) Immune Suppression during Oncolytic Virotherapy for High-Grade Glioma; Yes or No? J Cancer 6:203–217. [PubMed: 25663937]
20. Jang BS, Kim IA (2020) A Radiosensitivity Gene Signature and PD-L1 Status Predict Clinical Outcome of Patients with Glioblastoma Multiforme in The Cancer Genome Atlas Dataset. Cancer Res Treat 52:530–542. [PubMed: 31801317]
21. Wei J, Montalvo-Ortiz W, Yu L, et al. (2021) Sequence of αPD-1 relative to local tumor irradiation determines the induction of abscopal antitumor immune responses. Sci Immunol 6.
22. Williamson CW, Sherer MV, Zamarin D, et al. (2021) Immunotherapy and radiation therapy sequencing: State of the data on timing, efficacy, and safety. Cancer 127:1553–1567. [PubMed: 33620731]
23. Xia W, Zhu J, Tang Y, et al. (2020) PD-L1 Inhibitor Regulates the miR-33a-5p/PTEN Signaling Pathway and Can Be Targeted to Sensitize Glioblastomas to Radiation. Front Oncol 10:821. [PubMed: 32537433]
24. Li G, Wang Z, Zhang C, et al. (2017) Molecular and clinical characterization of TIM-3 in glioma through 1,024 samples. Oncoimmunology 6:e1328339. [PubMed: 28919992]
25. Li X, Wang B, Gu L, et al. (2018) Tim-3 expression predicts the abnormal innate immune status and poor prognosis of glioma patients. Clin Chim Acta 476:178–184. [PubMed: 29174343]

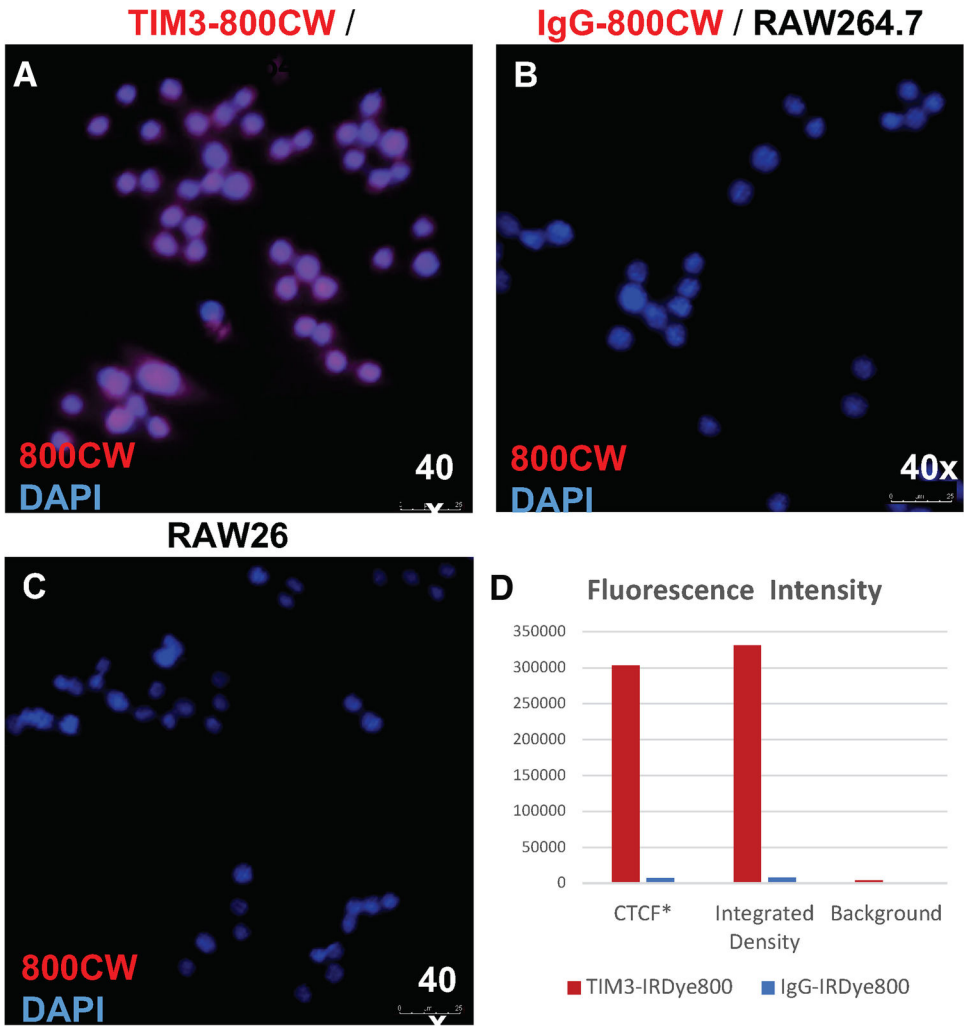

Figure 1.

Immunofluorescence microscopy of RAW 264.7 macrophages following conjugate labeling with **(a)** TIM3-800CW. Controls were labeled with **(b)** IgG-800CW and **(c)** DAPI-only. Images obtained with objective 40, numerical aperture 0.8. **(d)** Quantification of mean fluorescence intensity of 800CW from single cells segmentations (N = 10 per group). Intensity was measured by the calculated total cell fluorescence (CTCF), calculated as: mean integrated density – (area * mean background).

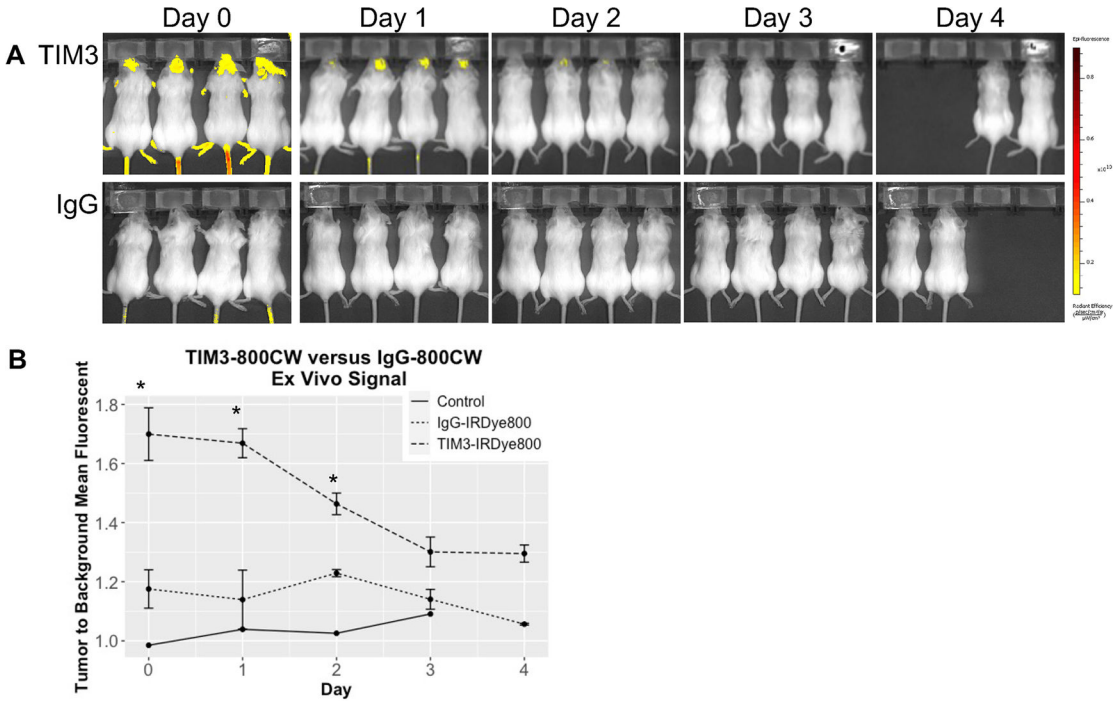

Figure 2.

(a) Interval IVIS Spectrum images obtained at excitation and emission of 745 and 800 nm, small binning, f-stop 2, and 3 seconds of exposure. **(b)** Line graph of fluorescent signal in vivo for mice injected with TIM3-800CW and IgG-800CW conjugate. Mean fluorescent signal was measured by ratio of the brain tumor region of interest and normal tissue. *p < 0.05

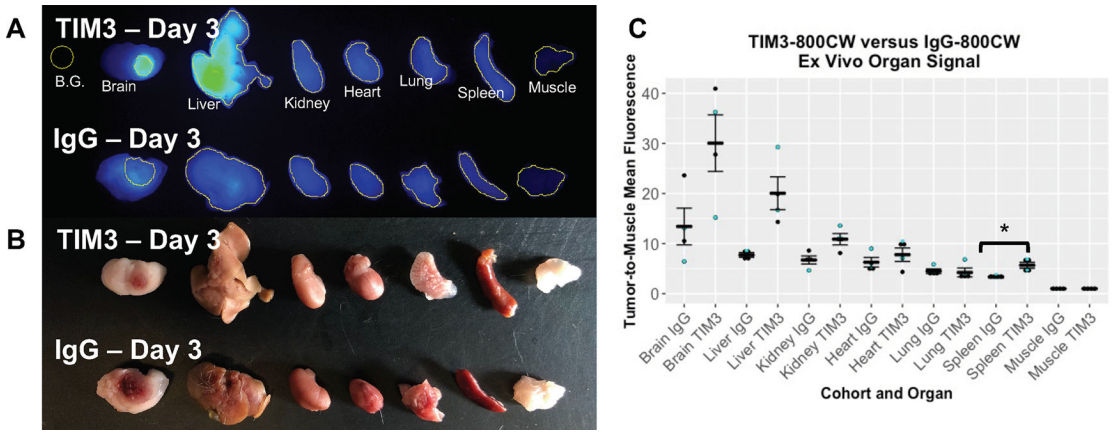

Figure 3.

Representative ex vivo **(a)** fluorescent and **(b)** brightfield imaging of organs from mice treated with either TIM3-800CW (N=4) or IgG-800CW (N=4). **(c)** Dot plot summarizing the average mean fluorescent intensities of organs and their respective standard errors. Organs were collected from Day 3 (cyan dot) and 4 (black dot) of the in vivo trial. *p < 0.05

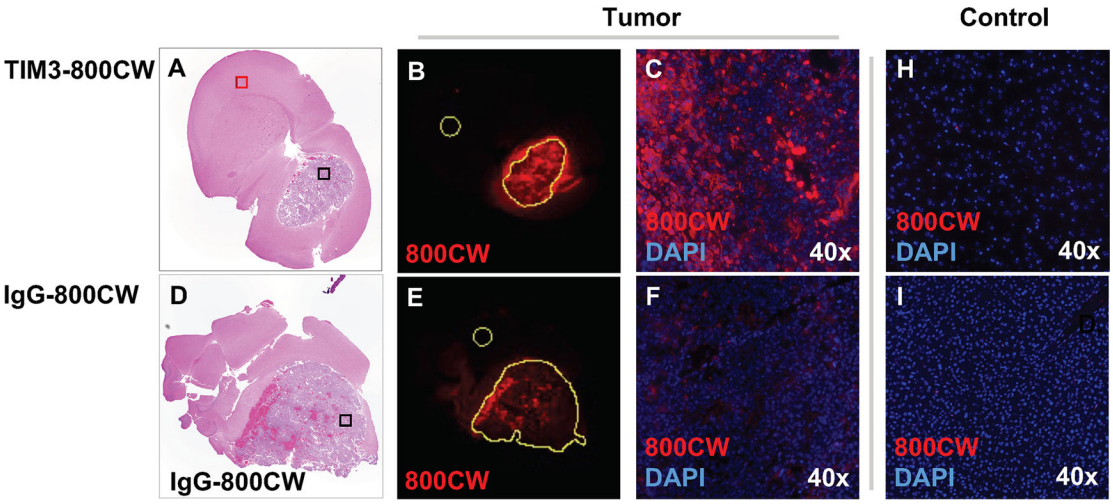

Figure 4.

Histologic mouse brain sections from a mouse treated with **(a-c)** TIM3-800CW and **(d-f)** IgG-800CW conjugates. Low power view using near infrared imaging **(b, e)**. of tumor area for TIM3-800CW versus IgG-800CW (excitation/emission 785/820 nm, resolution = 21 μm). Signal intensities were measured based on segmentations of the corresponding areas of hematoxylin and eosin. These were normalized to contralateral brain (yellow circles). High power view using near infrared imaging **(c, f)** with DAPI counterstain depicts cellular uptake of TIM3-800CW in tumor. Additional high-power field of controls of **(h)** contralateral brain (red square), and **(i)** liver for a mouse treated with TIM3-800CW. Images obtain with objective 20, numerical aperture 0.75.